Horizontal Stratification during Deep Convection in the Labrador Sea

Eleanor Frajka-Williams, *

University of Southampton, Southampton, UK

Peter B. Rhines, and Charles C. Eriksen

University of Washington, Seattle, WA

Corresponding author address: Eleanor Frajka-Williams, National Oceanography Centre, University of Southampton Waterfront Campus, Southampton, UK.

E-mail: e.frajka-williams@soton.ac.uk

ABSTRACT

Deep convection—the process by which surface waters are mixed down to 1000 m or deeper—forms the primary downwelling of the meridional overturning circulation in the northern hemisphere. High resolution hydrographic measurements from Seagliders indicate that during deep convection—though water is well-mixed vertically—there is substantial horizontal variation in density over short distances (tens of kilometers). This horizontal density variability present in winter (Jan–Feb) contains sufficient buoyancy to restratify the convecting region to observed levels 2.5 months later, as estimated from Argo floating platforms. These results highlight the importance of small-scale heterogeneities in the ocean which are typically poorly represented in climate models, potentially contributing to the difficulty climate models have in representing deep convection.

1. Introduction

Deep convection occurs when intense wintertime heat fluxes cool weakly stratified surface waters, resulting in well-mixed surface layers 100s of meters thick. In the Labrador Sea, the major region for open ocean deep convection in the northern hemisphere, cyclonic circulation reduces the surface stratification, while cold, dry winds from over Canada and Siberia cool the ocean (Lazier et al. 2002). This cooling increases the density of the surface water, allowing it to sink in plumes with narrow horizontal scales (100 m) and fast vertical speeds (up to 10 cm s^{-1}), mixing waters down to 1000 m or more (Lilly et al. 1999; Steffen and D'Asaro 2002). During periods of deep convection, density differences between the surface and the base of the mixed layer are small by definition (less than 0.01 kg m^{-3}) (Lazier et al. 2002). When surface buoyancy losses no longer exceed the lateral input of buoyant waters from surrounding regions, the area again becomes stratified with light waters overlying denser waters, via some process of restratification (Marshall and Schott 1999).

While observations have established that convection has a fine-scale texture and restratifies rapidly to a state with strong 'spice' (where temperature and salinity, T and S, variability are nearly compensating in density), (Lilly et al. 1999), restratification timescales in models are longer (for example, Jones and Marshall (1997); Katsman et al. (2004)). These numerical studies used a simplified initial density state, either a pre-convection state with horizontal isopycnals (Visbeck et al. 1996), or a central well-mixed (horizontally and vertically) column of convected water in a so-called "cylinder collapse" experiment (Jones and Marshall 1997). While the numerical modelling study of Legg and McWilliams (2000) allowed for heterogeneous properties, they found that T and S were largely compensating in density.

The longer, annual timescales of restratification require lateral inputs of buoyant water from the boundary currents to maintain observed heat and salt budgets in the Labrador Sea (Straneo 2006; Schmidt and Send 2007). Recirculating boundary currents have been observed using floats (Lavender et al. 2005), while eddy-fluxes have been the focus of several more recent papers. The flux of buoyant waters has been divided into fluxes by three classes of

eddies in recent numerical modelling studies (Chanut et al. 2008; Gelderloos et al. 2011). The three types are the Irminger rings formed by instability at Cape Desolation, boundary current eddies spawned by instabilities of the boundary current, and convective eddies generated by baroclinic instability of the steep isopycnal slopes formed during deep convection. While the results suggested different eddy processes were dominant in the two model studies, both focus on the necessity of bringing buoyancy to the convective region in order to increase stratification before the following year's deep convection. They are not, however, the same processes which control the immediate restratification after deep convection.

For immediate restratification, lateral gradients in mixed layer density are susceptible to baroclinic instability. These instabiliities grow eddies which can restratify the mixed layer over a single day (Boccaletti et al. 2007). Observations have demonstrated horizontal gradients in mixed layer density (Cole et al. 2010; Timmermans et al. 2012), while numerical modelling in the North Atlantic, showed that such instabilities speed up restratification relative to that by surface warming alone (Mahadevan et al. 2012).

In this study, we present hydrographic observations of deep convection (>1000 m deep mixed layers) from autonomous underwater gliders. We find that the convective region consists of patches of vertically well-mixed water within a several 100 km-wide region, with temperatures and salinities that vary in the horizontal direction. We find that while T and S are compensating to a degree, there are considerable horizontal gradients in density. This paper will demonstrate that horizontal density variations during the convection period are sufficient to account for post-convection vertical stratification.

2. Data

Data used here are from two sources: Seaglider autonomous underwater vehicles and Argo profiling floats. Seagliders profile in a sawtooth pattern from the surface to 1000 m depth with an approximate 1:3 vertical to horizontal slope. Each dive "cycle" consists of a down

profile and up profile which takes roughly 9 hours to complete, over a horizontal distance of 6 km. During a single cycle, temperature, conductivity and pressure are measured at intervals of 0.3 to 2.4 m. The gliders used here (designated sg014 and sg015) were deployed in the Davis Strait in Sep 2004, crossed Arctic watermasses and traveled south to the region of deep convection in January 2005. Sg014 and sg015 collected 41 and 59 profiles, respectively, of fully convecting water (mixed layer depths exceeding 700 m, Fig. 2c) and vertical velocities up to 10 cm s^{-1} (Frajka-Williams et al. 2011).

Hydrographic data from Seagliders were first binned into 2 dbar intervals, and then linearly-interplated across bins where there were no data (at depth) onto an evenly spaced 2 dbar grid. Argo float profiles were coarser than 2 dbar throughout, and so were linearly-interpolated onto a regularly spaced 2 dbar grid.

Due to the slow speeds of Seaglider (about 20 cm s^{-1} through water), temporal variations may be aliased into horizontal variability. Seagliders were only in the convection region for a few weeks before they returned north for intended recovery offshore Nuuk, Greenland. To separate some of the space-time variability, we also analysed the evolution of temperature and salinity in the convection region from Argo float profiles. An individual Argo float profiles from 2000 m to the surface every 10 days. The vertical resolution of the floats used here was about 70 samples per 2000 m and in the convecting region (here, we use 56.3–59°N and 50–55.5°W). 36 quality-controlled profiles were available in this box from 1 Jan–1 Jun 2005, with 9 profiles showing a well-mixed surface layer deeper than 700 m.

Heat fluxes are from an assimilating model product, the NCEP/NCAR Reanalysis II six-hourly product, which show reasonable variability for the region, though biased due to the small number of observations available to correct the model (Renfrew et al. 2002).

We use two measures to describe stratification. The first is a more qualitative indicator: the standard deviation of density in a single profile. For Fig. 3, the density anomaly is calculated relative to the mean potential density (σ_1) of 1032.33 kg m^{-3} for the convecting region measured by gliders. The standard deviation of density anomaly for a profile is an

indicator of how well-mixed the profile is (a small standard deviation is vertically well-mixed, while larger standard deviation is associated with a more stratified profile, due to the density change between the light surface waters and dense deeper waters). For a more quantitative measure, the stratification can be estimated as the amount of buoyancy that must be removed (e.g. through surface fluxes during convection) in order for the water column to mix down to a depth h with subsequent uniform density. This quantity is called convection resistance and is defined as

$$CR(h) = \int_{-h}^{0} \sigma_1(S, \theta, z) dz - h\sigma_1(S, \theta, h) \tag{1}$$

with units kg m^{-2}, which scales with buoyancy (Bailey et al. 2005). (Multiplying by gravitational acceleration gives units of kg m^{-1}s^{-2} or energy per unit volume.) In this formulation, a stratified water column will have negative CR while a well-mixed water column has a CR of zero. Unstable stratification would have a positive CR, with dense water over light. Unstable stratification could be present briefly during deep convection, but would rapidly overturn, mixing down to the convection depth.

From the hydrographic profiles and also as later observed in the convection resistance profiles, we find well-mixed profiles to 700 or more meters deep; in some cases to the full depth of the 1000 m observable by Seaglider. However, other profiles, both from Seaglider and Argo show property and density variations at 800 or 900 m. Since our discussion concerns active deep convection, we choose a fixed limit of 700 m for the lower limit of integration in later calculations of stratification. Below this depth, several profiles become stratified. In calculating convection resistance, the contribution by this deep stratification would be indistinguishable from profiles with a stratified surface layer and weakly stratified deeper layer.

3. Convective hydrography

During deep convection, surface heat fluxes exceeded 1000 W m^{-2} and winds exceeded 25 m s^{-1} (not shown), driving buoyancy-driven overturning and turbulent mixing. Near the peak of convection as observed by the gliders, Seaglider profiles from 25 Jan–13 Feb showed surface to 1000 m density (σ_1) ranges of less than 0.01 kg m^{-3} (Fig. 2c). Within this patch of vertically well-mixed profiles however, mixed-layer averaged temperatures and salinities ranged from 3.34–3.6°C and 34.83–34.86, respectively (Fig. 2a, b). While temperature and salinity were partially compensated—where density variations due to temperature cancelled variations due to salinity (warmer but saltier, or colder but fresher)—the observed potential density (σ_1) in the convection region ranged from 32.323–32.343 kg m^{-3}. These ranges represent the maximal range of salinity, potential temperature and potential density for glider mixed layer properties, from profiles where mixed layer depths were deeper than 700 m.

While the profiles show a large range in properties and densities, they do not indicate whether the variations are part of a background gradient in space or time, or fluctuations in values as the glider progresses through the convecting patch. To evaluate the spatial-temporal evolution of density, salinity and temperature, we calculate the mean and standard deviation of density for each profile, plotted against time and space (Fig. 3).

While the standard deviation is low for an individual profile, indicating well-mixed profiles, the changes in mean density between profiles is substantial (on the order of 0.01 kg m^{-3}). We note that sg015 shows a reduction in density between 25–29 Jan, and a subsequent increase from 2–9 Feb. Sg014, on the other hand, shows an increase in density between 28 Jan–1 Feb, and a reduction from 1–5 Feb. The profile-averaged density anomaly has a local maximum on 30 Jan and local minimum on 8 Feb with a difference of 0.026 kg m^{-3}. From 28–29 Jan, over 3 dive cycles (6 profiles $\approx$ 15.1 km over ground), density changes by 0.010 kg m^{-3}. Similar changes of 0.010 kg m^{-3} were observed from 3–4 Feb over 5 profiles (13.9 km over ground).

Overall, there is no monotonic tendency in the glider data towards denser water, as might be expected if the gliders were observing purely temporal evolution. Considering temperature separately, we see a change from colder to warmer waters in sg015 data as observations measure lighter water, followed by a change towards colder waters. Since the heat flux over these periods was net cooling of the ocean (Fig. 4), in a 1-dimensional, temporal evolution of the profile, we would expect to see only cooling of water temperatures. Since the cooling is due to cold, dry air off of Siberia and the Canadian archipelago, we might further expect concurrent evaporation. Instead, we see changes of observed temperatures from warmer to colder with salinity changes from saltier to fresher. Together, these show that the variations in properties through the actively convecting patch must be at least partially due to horizontal variations in properties rather than purely temporal evolution.

Nine profiles from Argo floats show well-mixed layers deeper than 700 m (Fig. 2). The profile locations tended to be in the south and southeast portion of the region of interest, whereas Seaglider data were more northerly. In addition, the Argo float data were from late January through mid-March, potentially seeing more fully-developed deep convection. Indeed, in comparing the Argo profiles to Seaglider data, the Argo data span about half the density (temperature, and salinity) range as that seen by Seagliders. They also tend towards denser, colder, and fresher than the bulk of the Seaglider data. It is interesting to note, however, that while the Argo float profiles included data past the observational period of the gliders, there is still no bulk change from the Argo profiles in 25 Jan–13 Feb towards colder and denser profiles in the 14 Feb–15 Mar period.

While both these pieces of evidence may indicate striking spatial variability in watermass properties and density during deep convection, we do not expect the observed variability to be entirely due to spatial variations. Over the 2.5 weeks of glider observations, we expect convective processes to vary on short (1-day) timescales (Frajka-Williams et al. 2011), as vertical velocities respond to changes in heat flux within 1-day. Convection is a process of surface cooling, sinking of newly-densified waters, and horizontal slumping across the subse-

quent lateral gradients in density on short time scales. Even so, based on these observations showing non-monotonic changes in density across short spatial scales and in the absence of a more complete dataset, we will make the assumption that the glider data are a representative snapshot of active convection, and will treat the variations in properties as spatial-only. The limited extent of glider data suggests that the observed variations form a lower bound to density variations that may have been observed during this time period (late January to mid-February) given a more complete coverage of the convective patch.

4. Evolution of stratification

The evolution of convection can be seen in the Argo profiles of density, with an increase in surface density to a maximum in mid-February and mid-March (Fig. 4c). In late March, one of the Argo floats observed properties within an eddy with a cold, fresh surface layer, though the other float in the region also showed restratification. (In the depth-time swath in Fig. 4c, these two floats are interspersed in time, suggesting temporal variability, but because they are in two different parts of the region, the variations are due to one float being within an eddy, and the other without.) Stratification continues to increase as thermal warming shows a net heating of the oceans (Fig. 4a).

Post deep convection, an Argo hydrographic profile from 23 Mar (not in an eddy) showed a density difference of 0.015 kg m^{-3} from the surface to 700 m. This is immediately after the surface has restratified. This vertical density difference is of similar magnitude to the horizontal variations in density observed by sg015 (e.g., from 29 Jan–7 Feb, 8 days and 100 km, sg015 sees a horizontal range of 0.02 kg m^{-3}). Vertical density variations the same order of magnitude as horizontal are not common, and already hint at the potential contained by the horizontal variations in the glider data. However, using density difference as a metric does not fully capture the stratification in the water column. For the 23 Mar profile, some of this density difference can be accounted for by a buoyant layer at the surface. The surface

to 700 m convection resistance for 23 Mar is $CR(700) = -5.5$ kg m^{-2}, which is outside the mean and standard deviation of the CR(700) from glider profiles during deep convection of -1.4 ± 2.1 kg m^{-2} (excluding the 12 profiles in the stratified eddy). The overall range in $CR(700)$ from Argo floats is from 0 to -10 between 6 Feb and 27 Apr.

In April, there is a change in sign of surface heat flux from positive (cooling of the ocean) to negative (warming of the ocean, Fig. 4a). This is followed by an increase in the temperature contribution to stratification (not shown). The magnitude of convection resistance increases to < -5 kg m^{-2}, more negative than the convection resistance estimates from deeply convecting Seaglider profiles. From Argo hydrographic profiles, the profile of CR referenced to 700 m indicates low stratification, near-zero CR on 6 Feb (0.01 kg m^{-2}) while on 4 May, in restratified water, the CR becomes more negative (-12.5 kg m^{-2}).

5. Buoyancy content during convection vs restratified waters

In the previous section, we compared the $CR(700)$ values from Argo to those from Seaglider, where in both cases, the CR was referenced to the density at 700 m for that profile. We now average together profiles of $CR(z)$ referenced to each depth, to create a convective-patch average of CR (see Fig. 5, black with shading to indicate the standard deviation at each depth). The result indicates low stratification, with an average CR(700) near-zero (-1.4 kg m^{-2}). The profiles of CR confirm what was visible in the property profiles (Fig. 2a–c): that individual profiles are vertically well-mixed.

Now, to quantify the overall buoyancy available in the convecting region, allowing for spatial variations in density, we will reference CR to the same density for each profile. We are assuming that the variations in density observed by Seaglider are due purely to horizontal variations rather than temporal variations (§3). We use reference values of $S_0 = 34.84$, $\theta_0 = 3.37$°C and $h = 700$ dbar, where S_0 and θ_0 were mean values of salinity and

temperature in the top 700 m during deep convection from 27 Jan–26 Feb in Argo data. The observed convecting state was horizontally-stratified but vertically well-mixed, while the final state is now presumed to be relatively horizontally homogenous and vertically-stratified (Fig. 4c). To estimate the buoyancy available in the convecting region sampled by Seaglider, we adiabatically sort the density measurements into the state of lowest potential energy, with the densest measurements at the bottom (1000 m) of the measured volume along the Seaglider transect and the lightest at the surface. Given that the glider data were gridded onto a regular 2 dbar grid, the result is a set of the same number of profiles, now horizontally homogenous and vertically-stratified set of profiles. Averaging across this set, we then have a single profile representative of this sorted state. This offers an estimate of the bulk stratification of the convecting volume. From this single sorted density profile, we can then calculate a bulk convection resistance to represent the buoyancy available in the original profiles from the convecting region. For the sorted profile, the CR at 700 m is -8.3 kg m^{-2}. Thus, CR from the sorted Seaglider data matches (or is even more stratified than) the CR from 20 Apr from Argo ($CR(700) = -6.7$ kg m^{-2}, Fig. 4b). This indicates that from Seaglider observations during deep convection, there appears to be sufficient buoyancy available to restratify the region to observed April-levels of stratification.

Looking in more detail at the Argo data from 20 Apr, we see that this enhanced CR can be at least partially-attributed to a surface fresh layer (Fig. 4d). Comparing just the subsurface stratification, we find that the profile of CR from 4 May is quite similar to that of the sorted glider data (Fig. 5). In particular, by shifting the $CR(z)$ from 4 May to match that of the sorted glider profile at 700 m, the profile of CR between 100 m and 700 m closely resembles that of the sorted glider profile. The offset difference between 100 and 600 m can be explained by where the CR profiles had stronger slopes (indicating stronger stratification). In the Argo profile between 100 and 400 m, there was slightly stronger stratification than the sorted glider profile, while the sorted glider profile had increased stratification between 500 and 650 m. The Argo profile shows quite strong stratification at 80–100 m where the

transition between the surface buoyant layer and more weakly stratified subsurface layer occurs.

Our method of comparing a sorted glider profile to the Argo profile assumes that the restratification of the glider data is purely adiabatic. By comparing the sorted profile with Argo data, we are further assuming that the two datasets are representative of the same volume of water. If this were the case, then the volume of water in a particular $\theta - S$ class would not change from the convecting period to the restratified profile on 20 Apr. To check this, the volumetric $\theta - S$ diagram was calculated from the Seaglider data (25 Jan–13 Feb) in bins of 0.002 and 0.01°C (See Fig. 6). The Argo profiles from 13 Apr to 4 May suggest that while the bulk of the water did not change in salinity, from the Seaglider observations to the Argo profile, the temperature continued to cool. This is indicated by the absence of Argo temperatures above about 3.5°C. In addition, in the Argo profiles, there is a 50–100 m surface layer with very fresh ($S < 34.8$) and cold ($\theta < 3.4$°C, except 4 May, where $\theta \approx 3.54$°C) temperatures.

The temperature difference between the Argo profile and the largest volumes of convecting water in the Seaglider data may be attributed to the fact that the Seaglider left the region before the deepest mixed layers were observed (Fig. 4c). Indeed, the Argo floats show vertically-homogenous profiles through mid-March, while the gliders moved out of the convection region in mid-February. While from mid-February to mid-March, the Argo profiles do not show a continued trend towards colder or denser convecting water (Fig. 5d), the glider observations from late January to mid-February were warmer, on average, than in mid-February. This suggests that while gliders clearly observed active, deep convection with vertically well-mixed profiles from late January (near-zero CR, Fig. 4b), the properties of the convecting water did gradually cool until mid-February, when they appear to stabilize. This potential continued cooling may have been accompanied by additional horizontal homogenization (not observable with the present dataset). If this was the case, then the estimates of horizontal density variability from the Seaglider data may be an overestimate

of the buoyancy available immediately prior to restratification.

The fresh surface layer visible in the $\theta - S$ diagram of the Argo profile indicate that the fresh layer must have been imported to the region, as water this low in salinity is not present in the glider observations. Even so, the convection resistance in the 4 May Argo profile is dominated by stratification below 100 m, which matches the convection resistance in the sorted Seaglider profile (Fig. 5).

6. Discussion

Seaglider observations in Jan–Feb 2005 from a deep convecting patch within the Labrador Sea show vertically well-mixed profiles of temperature, salinity and density. However, over the 350 km wide patch observed by sg015 and 250 km by sg014, glider data exhibited substantial density variations between the vertically well-mixed profiles. In the case of sg015, variations were as much as 0.026 kg m^{-3} over just 9 days, or a density difference of 0.01 kg m^{-3} across 15 km horizontally. These density differences are similar to those used to determine how well-mixed a profile is, where the threshold of 0.01 kg m^{-3} in density is a common choice in the vertical for determining the mixed layer depth in the Labrador Sea. While the convecting region was observed over a span of 2.5 weeks (late January–mid-February), and from Argo float profiles we find that convection proceeded beyond the time that the gliders were there (through mid-March), the observed variations in temperature and density do not indicate a monotonic change towards denser and colder waters, as might be expected of a purely temporal change due to the net cooling by the atmosphere.

Based on these observations, we treat the observations from Seaglider as purely spatially-varying, while in reality, they will be a mix of spatial and temporal variations. Under this assumption, by comparing the buoyancy available in the convecting volume from Seagliders (late January to mid-February), with an estimate of buoyancy in restratified profiles from Argo in the same region, we find that the buoyancy available due to lateral variations in

density is sufficient to restratify the region to the observed stratification in April. If we further exclude the fresh surface layer from Argo profiles, then the convecting profiles from Seaglider show stratification similar to that from Argo data in May.

These finescale lateral heterogeneities in density may contribute to the difficulty that climate models have in representing convection and restratification. The Seaglider observations show non-negligible density differences on the scale of 10s of kilometers, while most climate models tend to be run at 100 km scales. In addition, the density overturns that cause convection invalidate the hydrostatic assumptions of models (that profiles are stably stratified). As a consequence, convection is often too deep or too persistent in numerical models. Numerical studies have investigated restratification processes, involving lateral fluxes of buoyant waters from outside the convection region (Katsman et al. 2004; Jones and Marshall 1997; Chanut et al. 2008; Gelderloos et al. 2011), but typically considering longer, annual timescales.

The immediate cessation of convection is likely to be enhanced or enabled by the density variations within the convecting patch, without invoking lateral fluxes from further away. Recent observations and simulations in the nearby Irminger Sea found that mixed layer eddies were responsible for the short timescale of restratification, prior to thermal warming (Mahadevan et al. 2012). These observed density variations may reduce the time to restratification, ending convection sooner and changing the estimates of deep water formation volume and properties.

Acknowledgments.

E. F. was supported by an NSF graduate research fellowship for a part of this work. Seaglider missions in the Labrador Sea were funded by the US National Oceanic and Atmospheric Administration Arctic Research Office. Many thanks to Jonathan Lilly, Erik van Sebille, Eric Kunze, and Eric D'Asaro for helpful discussions.

REFERENCES

Bailey, D. A., P. B. Rhines, and S. Hakkinen, 2005: Formation and pathways of North Atlantic Deep Water in a coupled ice-ocean model of the Arctic-North Atlantic oceans. *Journal of Climate*, **25**, 497–516.

Boccaletti, G., R. Ferrari, and B. Fox-Kemper, 2007: Mixed layer instabilities and restratification. *Journal of Physical Oceanography*, **37**, 2228–2250, doi:10.1175/JPO3101.1.

Chanut, J., B. Barnier, W. Large, L. Debreu, T. Penduff, J. M. Molines, and P. Mathiot, 2008: Mesoscale eddies in the Labrador Sea and their contribution to convection and re-stratification. *Journal of Physical Oceanography*, **38**, 1617–1643, doi:10.1175/2008JPO3485.1.

Cole, S. T., D. L. Rudnick, and J. A. Colosi, 2010: Seasonal evolution of upper-ocean horizontal structure and the remnant mixed layer. *Journal of Geophysical Research*, **115**, C04 012, doi:10.1029/2009JC005654.

Frajka-Williams, E., C. C. Eriksen, P. B. Rhines, and R. R. Harcourt, 2011: Determining vertical velocities from Seaglider. *Journal of Atmospheric and Oceanic Technology*, **28**, 1641–1656.

Gelderloos, R., C. A. Katsman, and S. S. Drijfhout, 2011: Assessing the roles of three eddy types in restratifying the Labrador Sea after deep convection. *Journal of Physical Oceanography*, **41**, 2102–2119, doi:10.1175/JPO-D-11-054.1.

Jones, H. and J. Marshall, 1997: Restratification after deep convection. *Journal of Physical Oceanography*, **27**, 2276–2287.

Katsman, C. A., M. A. Spall, and R. S. Pickart, 2004: Boundary current eddies and their role in the restratification of the Labrador Sea. *Journal of Physical Oceanography*, **34**, 1967–1983.

Lavender, K. L., W. B. Owens, and R. E. Davis, 2005: The mid-depth circulation of the subpolar North Atlantic Ocean as measured by subsurface floats, *Journal of Physical Oceanography*, **52**, 767–785.

Lazier, J., R. Hendry, A. Clarke, I. Yashayaev, and P. Rhines, 2002: Convection and restratification in the Labrador Sea, 1990-2000. *Deep Sea Research I*, **49 (10)**, 1819–1835.

Legg, S. and J. C. McWilliams, 2000: Temperature and salinity variability in heterogeneous oceanic convection. *Journal of Physical Oceanography*, **30**, 1188–1206.

Lilly, J. M., P. B. Rhines, M. Visbeck, R. Davis, J. R. N. Lazier, F. Schott, and D. Farmer, 1999: Observing deep convection in the Labrador Sea during winter 1994/95. *Journal of Physical Oceanography*, **29**, 2065–2098.

Mahadevan, A., E. D'Asaro, C. Lee, and M. J. Perry, 2012: Eddy-driven stratification initiates North Atlantic spring phytoplankton blooms. *Nature*, **337**, 54–58.

Marshall, J. and F. Schott, 1999: Open-ocean convection: Observations, theory and models. *Reviews of Geophysics*, **37**, 1–64.

Renfrew, I. A., G. W. K. Moore, P. S. Guest, and K. Bumke, 2002: Comparison of surface layer and surface turbulent flux observations over the Labrador Sea with ECMWF analyses and NCEP reanalyses. *Journal of Physical Oceanography*, **32**, 383–400.

Schmidt, S. and U. Send, 2007: Origin and composition of seasonal Labrador Sea freshwater. *Journal of Physical Oceanography*, **37**, 1445–1454.

Steffen, E. L. and E. A. D'Asaro, 2002: Deep convection in the Labrador Sea as observed by Lagrangian floats. *Journal of Physical Oceanography*, **32**, 475–492.

Straneo, F., 2006: Heat and freshwater transport through the central Labrador Sea. *Journal of Physical Oceanography*, **36**, 606–628.

Timmermans, M.-L., S. Cole, and J. Toole, 2012: Horizontal density structure and restratification of the Arctic Ocean surface layer. *Journal of Physical Oceanography*, **42**, 659–668.

Visbeck, M., J. Marshall, and H. Jones, 1996: Dynamics of isolated convective regions in the ocean. *Journal of Physical Oceanography*, **26**, 1721–1734.

List of Figures

393 3 Mean mixed-layer density anomaly for each profile (black) with the standard
394 deviations ($\pm$) for the profile, calculated between the surface and 700 m,
395 marked as a vertical bar for sg015 (a) and sg014 (b). Anomalies are calculated
396 relative to $\theta = 3.5°C$, $S = 34.85$ and $\sigma_1 = 32.33$ kg m^{-3}. Positive anomalies
397 are less dense. Small standard deviations indicate a high degree of vertical
398 homogeneity. The temperature contribution to density ($\alpha\theta'$) is given by the
399 black open circle, and the salinity contribution ($-\beta S'$) by the grey open circle.
400 When the signs of the temperature and salinity contributions are opposites,
401 they are density compensating. When the sign of the temperature or salinity
402 contribution is the same as the density anomaly, they are controlling the
403 density. 22

404 4 Evolution of stratification. (a) Heat flux derived from NCEP reanalysis II in
405 the region. (b) Convection resistance from Seaglider sg015 (squares) and Argo
406 float profiles (circles) down to 700 m. Near zero values indicate well-mixed
407 profiles, while negative values indicate stratified regions. The red squares are
408 from a stratified eddy, surrounded by deep convection, and were excluded
409 from Fig. 5 in order for the conclusions to be more conservative. Colors for
410 Argo profiles indicated the time period. (c) Density evolution (σ_1) from Argo,
411 shaded. The dashed black line shows the period and depth range of the glider
412 observations. (d) Potential temperature profiles (θ) from Argo, shaded. The
413 inset map shows the location of Argo profiles. Note, the time-axis in all cases
414 has been stretched so that each profile is given equal weight in the figure, even
415 though they may be unevenly spaced in time. 23

5 Convection resistance profiles for Seaglider sg015 and Argo float. The thin black line (1) is the average (±standard deviation, shading) of convection resistance profiles from sg015 calculated within the convection region above the mixed layer depth. The solid gray line (2) is the convection resistance calculated from the resorted density profile of all sg015 densities within the mixed layers deeper than 400 m. The Argo profile plotted is from 4 May (grey dashed), offset by 4.28 kg m^{-2} to align at 700 m with the glider profile. The Argo float shows a similar degree of stratification between 100 and 800 m deep as the sorted glider profile. 24

6 Volumetric $\theta - S$ diagram from Seaglider sg015 data (25 Jan–13 Feb) in grey shading, where the numbers indicate meters of thickness of water within a particular 0.002 salinity and 0.01°C bin. Only profiles with mixed layer depths greater than 400 m were used (excluding the eddy from 10–12 Feb 2005). The contours are σ_1 at 0.01 kg m^{-3} intervals. The Argo float data are given by colored circles where each circle represents 50 m thickness of a water with the given average properties. The small scattering of circles at salinities less than 34.8 indicate that some freshwater has been imported to the region. It also suggests that temperatures continued to cool past when the glider was in the convecting region. 25

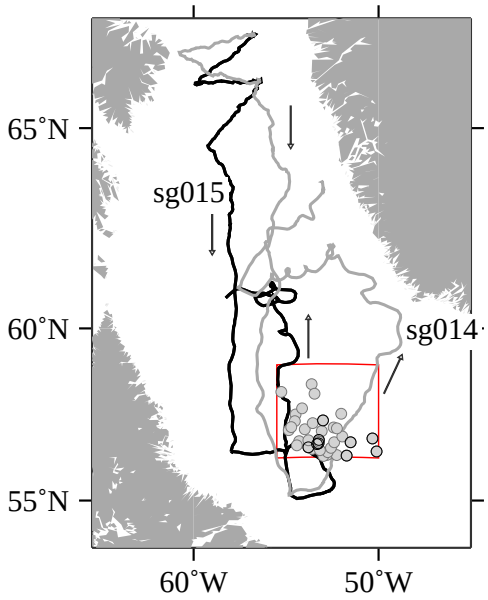

FIG. 1. A map of the Labrador Sea showing the glider and Argo profile locations. The Seaglider tracks are given by the lines (black, sg015; grey, sg014). 36 Argo float profiles were found in the box defined by 56.3–59°N, 50–55.5°W and the time period 1 Jan–1 May, 2005. Argo profiles locations are given by circles, where the grey circles are for the full period, and the black circles are the 9 profiles from Argo where the measured depth of the well-mixed surface layer exceeded 700 m. These 9 profiles were all from the period 25 Jan–15 Mar.

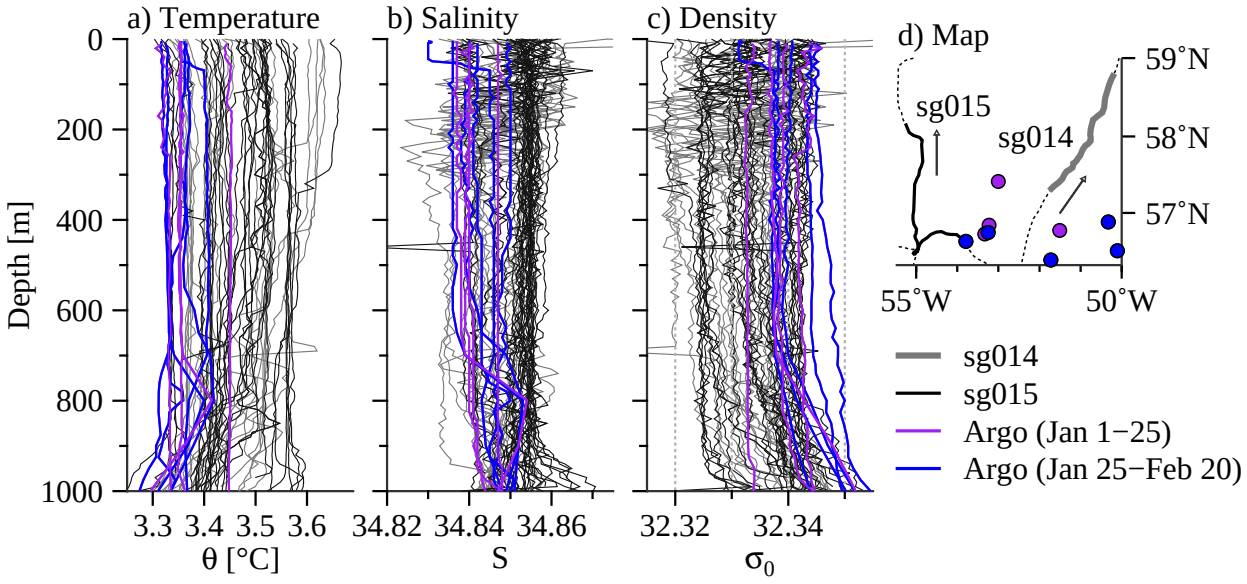

FIG. 2. Potential temperature (a), salinity (b) and potential density (σ_1) in kg m^{-3} (c) of 100 profiles during deepest mixed layers observed by sg015 (black), at the locations specified on Seaglider tracks in the inset map (d). Profiles in black and solid are from sg015 and grey from sg014, A total of 9 Argo float profiles from the period Jan 1–24 (5) are shown in purple, and 25 Jan–20 Feb (4) in blue. The full paths of both glider 14 and 15 are shown in dashed on (d) with the subset of profiles coming from the solid black transect (glider 15) and solid grey transect (sg014). The Argo float profiles are given by the colored circles.

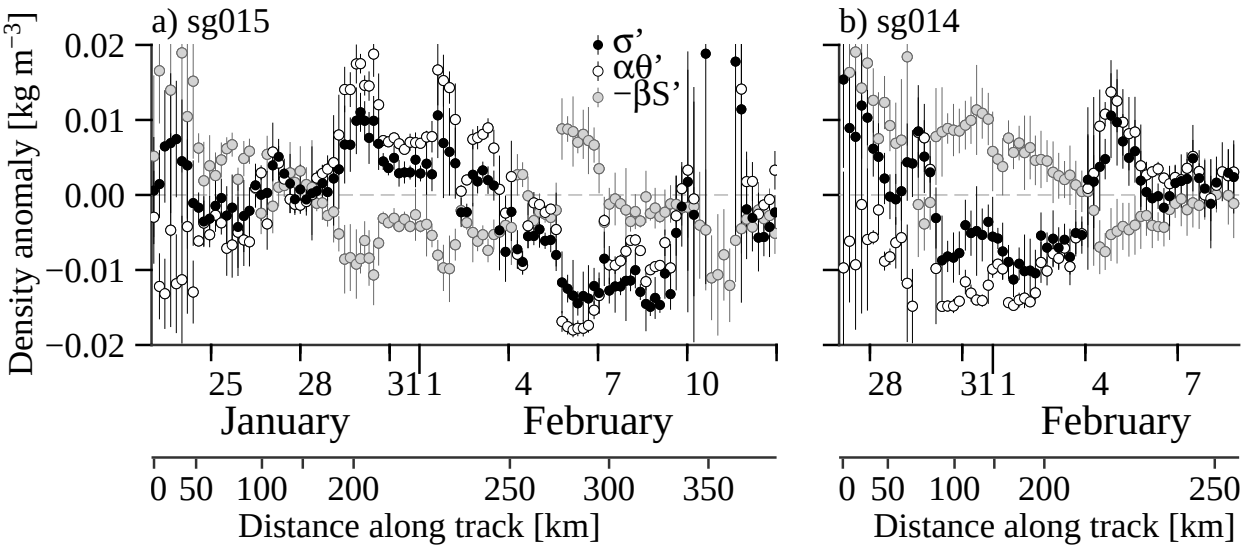

FIG. 3. Mean mixed-layer density anomaly for each profile (black) with the standard deviations ($\pm$) for the profile, calculated between the surface and 700 m, marked as a vertical bar for sg015 (a) and sg014 (b). Anomalies are calculated relative to $\theta = 3.5°\text{C}$, $S = 34.85$ and $\sigma_1 = 32.33$ kg m^{-3}. Positive anomalies are less dense. Small standard deviations indicate a high degree of vertical homogeneity. The temperature contribution to density ($\alpha\theta'$) is given by the black open circle, and the salinity contribution ($-\beta S'$) by the grey open circle. When the signs of the temperature and salinity contributions are opposites, they are density compensating. When the sign of the temperature or salinity contribution is the same as the density anomaly, they are controlling the density.

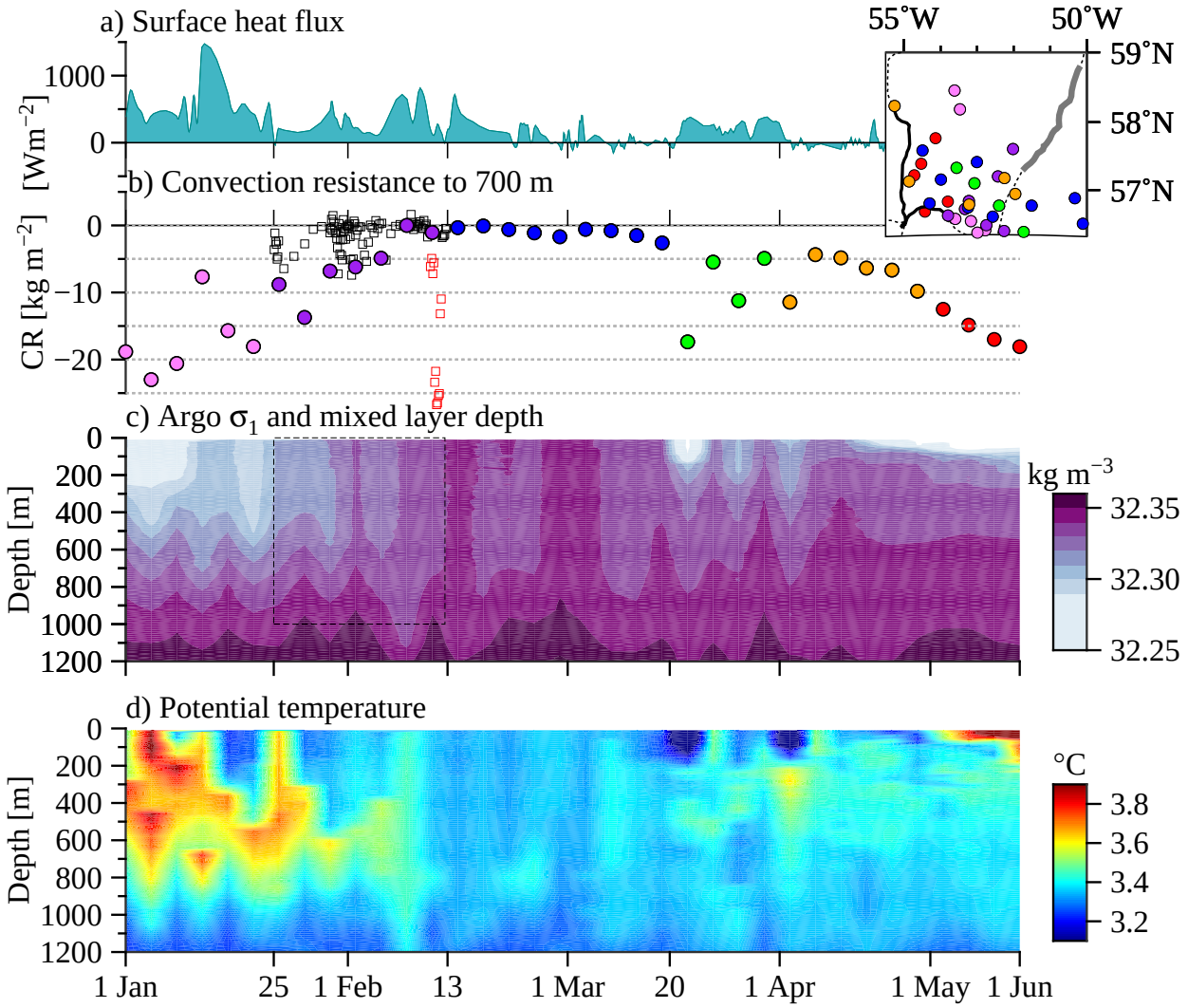

FIG. 4. Evolution of stratification. (a) Heat flux derived from NCEP reanalysis II in the region. (b) Convection resistance from Seaglider sg015 (squares) and Argo float profiles (circles) down to 700 m. Near zero values indicate well-mixed profiles, while negative values indicate stratified regions. The red squares are from a stratified eddy, surrounded by deep convection, and were excluded from Fig. 5 in order for the conclusions to be more conservative. Colors for Argo profiles indicated the time period. (c) Density evolution (σ_1) from Argo, shaded. The dashed black line shows the period and depth range of the glider observations. (d) Potential temperature profiles (θ) from Argo, shaded. The inset map shows the location of Argo profiles. Note, the time-axis in all cases has been stretched so that each profile is given equal weight in the figure, even though they may be unevenly spaced in time.

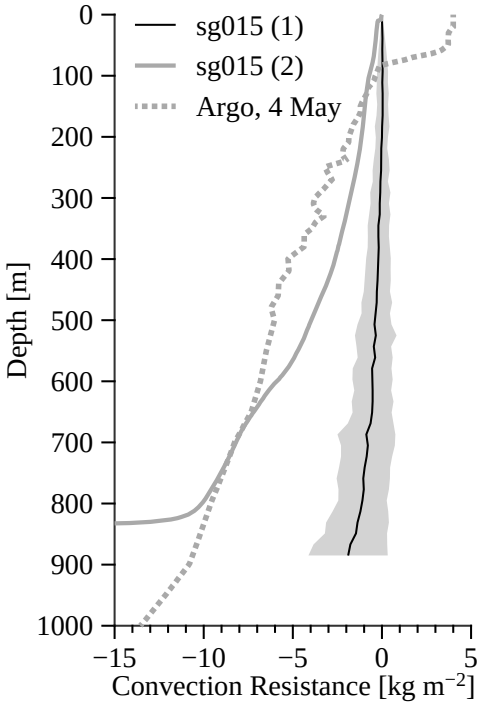

FIG. 5. Convection resistance profiles for Seaglider sg015 and Argo float. The thin black line (1) is the average (±standard deviation, shading) of convection resistance profiles from sg015 calculated within the convection region above the mixed layer depth. The solid gray line (2) is the convection resistance calculated from the resorted density profile of all sg015 densities within the mixed layers deeper than 400 m. The Argo profile plotted is from 4 May (grey dashed), offset by 4.28 kg m^{-2} to align at 700 m with the glider profile. The Argo float shows a similar degree of stratification between 100 and 800 m deep as the sorted glider profile.

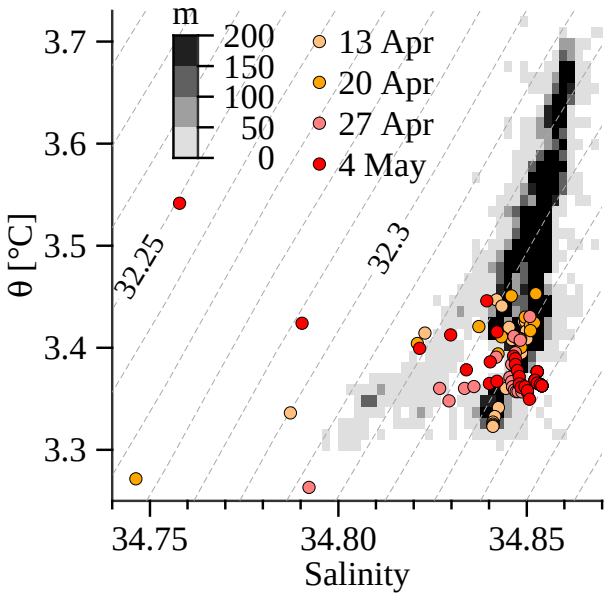

FIG. 6. Volumetric $\theta - S$ diagram from Seaglider sg015 data (25 Jan–13 Feb) in grey shading, where the numbers indicate meters of thickness of water within a particular 0.002 salinity and 0.01°C bin. Only profiles with mixed layer depths greater than 400 m were used (excluding the eddy from 10–12 Feb 2005). The contours are σ_1 at 0.01 kg m^{-3} intervals. The Argo float data are given by colored circles where each circle represents 50 m thickness of a water with the given average properties. The small scattering of circles at salinities less than 34.8 indicate that some freshwater has been imported to the region. It also suggests that temperatures continued to cool past when the glider was in the convecting region.